Contribution of groundwater discharge to the coastal dissolved nutrients and trace metal concentrations in Majorca Island: karstic vs detrital systems.

Antonio Tovar-Sánchez[1,2,*], Gotzon Basterretxea[3], Valentí Rodellas[4], David Sánchez-Quiles[2], Jordi García-Orellana[4,5], Pere Masqué[4,5,6], Antoni Jordi[3], José M. López[7], Ester Garcia-Solsona[4]

1. Department of Ecotoxicology, Ecophysiology and Biodiversity of Aquatic Systems, ICMAN (CSIC). Campus Universitario Río San Pedro, 11510 Puerto Real, Cádiz. Spain.
2. Department of Global Change Research. Mediterranean Institute for Advanced Studies, IMEDEA (UIB-CSIC), Miguel Marques 21, 07190 Balearic Islands, Spain.
3. Department of Ecology and Marine Resources. Mediterranean Institute for Advanced Studies, IMEDEA (UIB-CSIC), Miguel Marques 21, 07190 Balearic Islands, Spain.
4. Institut de Ciència i Tecnologia Ambientals, Universitat Autònoma de Barcelona, Bellaterra 08193, Spain
5. Departament de Física & Institut de Ciència i Tecnologia Ambientals, Universitat Autònoma de Barcelona, Bellaterra 08193, Spain.
6. School of Physics - Oceans Institute. The University of Western Australia, 35 Stirling Highway. CRAWLEY, WA 6009, Australia.

7. Instituto Geológico y Minero de España (IGME). Área de Infraestructura Hidrogeológica. Oficina de Proyectos de Palma de Mallorca, C/Ciudad de Queretaro s/n, 07007 Balearic Islands, Spain.

Corresponding Author

*Antonio Tovar-Sánchez. Department of Ecotoxicology, Ecophysiology and Biodiversity of Aquatic Systems, ICMAN (CSIC). Campus Universitario Río San Pedro, 11510 Puerto Real, Cádiz. Spain. Phone: +34 956832612. E-mail: a.tovar@csic.es

KEYWORDS: Groundwater, SGD, Majorca Island, trace metals, nutrients.

Abstract

Submarine groundwater discharge (SGD) derived nutrient (NO_2^-, NO_3^-, NH_4^+, PO_4^{3-}, and SiO_2) and trace element (Cd, Co, Cu, Fe, Mo, Ni, Pb, V and Zn) loadings were systematically assessed along the coast of Majorca Island, Spain.. Groundwater, Ra, nutrient and metal fluxes were assessed in a general survey around the island and in three representative coves during 2010. We estimated that brackish water discharges through the shoreline are important contributors to the DIN, SiO_2, Fe and Zn budgets of the nearshore waters. Furthermore, our results showed that SGD-derived elements are conditioned by the hydrogeological formations of the aquifer and discharge type. Thus, while rapid discharges through karstic conduits are enriched in SiO_2 and Zn, the large detrital aquifers of the island typically present enhanced concentrations of Fe. The estimated total annual inputs of chemicals constituents discharged by SGD to the coastal

48 waters were: DIN: 610 10^3 kg yr^{-1}, SiO_2: 1400 10^3 kg yr^{-1}, Fe: 3.2 10^3 kg yr^{-1} and Zn: 2.0

49 10^3 kg yr^{-1}. Our results provide evidence that SGD is a major contributor to the dissolved

50 pool of inorganic nutrients and trace metals in the nearshore waters of Majorca.

51

52

53

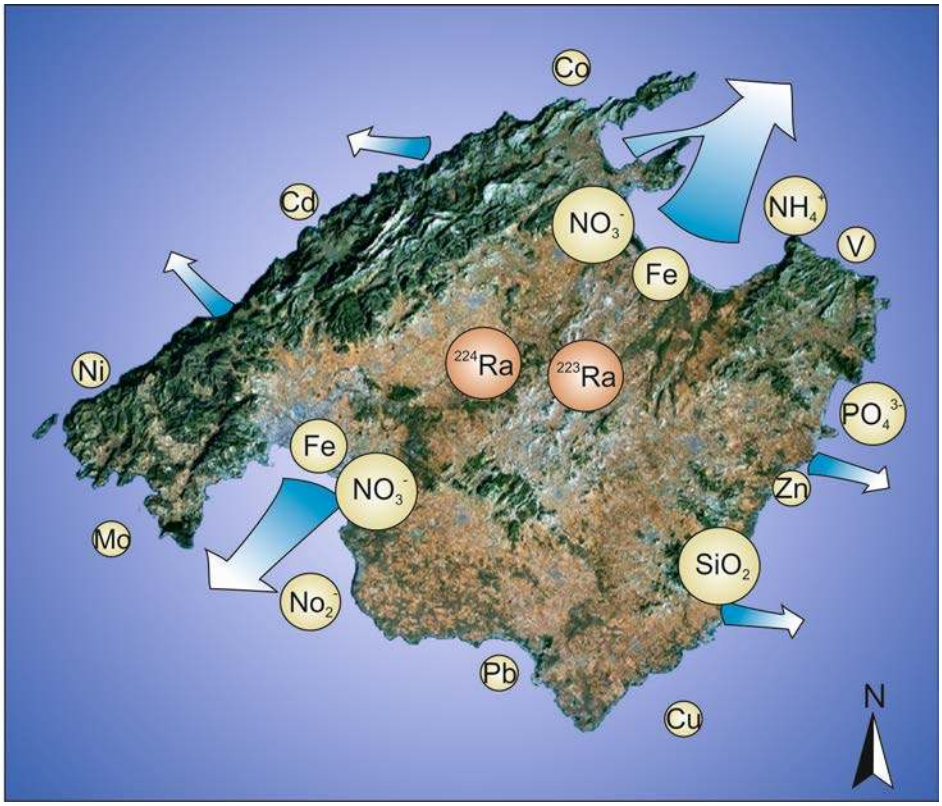

54

Introduction

The distribution and abundance of phytoplankton biomass and net primary production in the ocean is regulated by the availability of light and nutrients (mainly N, P, Fe), by physical processes of ocean circulation, mixed-layer dynamics, upwelling, atmospheric dust deposition, and the solar cycle[1]. The net primary production in the open waters of the Mediterranean Sea is primarily regulated by nutrient supply through vertical mixing[2]. Conversely, in the coastal waters and more particularly, in the nearshore waters of this oligotrophic sea, a large proportion of the marine productivity is regulated by the supply of 'new' solutes from land sources rather than by recycling or by vertical mixing[3]. Although river outflow has traditionally received most attention as the main pathway of nutrient and other element export from land, growing evidence demonstrates that significant delivery of terrestrial compounds can be also channeled through submarine groundwater discharges (SGD). SGD is known to deliver nutrients, metals and other land-derived compounds to the coastal ocean[4–6] and growing evidence demonstrates that this submarine source is playing a key role in the sustainment of coastal ecosystems[7–10]. This may be particularly relevant in arid and semi-arid regions with scarce riverine outflow and in oligotrophic seas like the Mediterranean, where the mean annual contribution of SGD has been estimated to be in the range of 300 - 50000 km^3yr^{-1} and could constitute a major source of terrestrial compounds to the overall budgets[11,12].

The geological characteristics of a given aquifer and its associated water flow, together with the human activities influencing its dynamics, determine the major aspects of the chemical composition of SGD. For example, karstified carbonate aquifers can exhibit rapid response to rainfall due to their underground structures of fractures and preferential conduits that can rapidly transfer the infiltrated water into the sea. Therefore,

79 residence time of groundwater in this type of aquifers is generally short, yielding greater
80 flow than surface runoff[13]. Karst systems are also particularly vulnerable to pollution
81 (such as agriculture) because of focused infiltration and rapid contaminant transport in
82 the phreatic zone[14]. Karst conduits are a primary source of fresh groundwater[15,16];
83 nevertheless, the ecological significance of these discharges linking continental and open
84 seawaters is generally very localized, and the environmental effects of karst discharges
85 are more perceptible in nearshore locations, such as bays, coves and semi-enclosed areas,
86 where the dilution due to mixing with open waters are reduced.

87 SGD usually occurs as a slow and diffuse flux through permeable sediments in the
88 nearshore[17]. Flow through detrital granular media is generally much slower and is driven
89 by hydraulic gradients, and a number of forcing mechanisms which regulate the flux of
90 new and recycled nutrients to seawater, fuelling and maintaining primary production[18].
91 Contrastingly with karst discharges, flow through porous media (as the case of detrital
92 zones) allows for a higher degree of interaction between water and substrate, favoring ion
93 exchanges. Flow in permeable coastal sediments includes an important component of
94 recirculated seawater, which can comprise a high percentage of the total SGD flux[19].
95 Indeed, the mixing area between fresh and salty water in the coastal boundary of these
96 aquifers is defined as a subterranean estuary[20], and is an area of intense geochemical
97 transformations[21,22].

98 Previous studies conducted in Majorca Island indicate that SGD is ubiquitous
99 around the island representing a major vector of CO_2, nutrients and Fe to the coastal
100 waters[9,10]. However, the magnitude of the global SGD-driven of nutrients and trace
101 metals to the coastal waters of Majorca Island is not yet well established. In this island,

both karst and detrital coastal aquifers are clearly identified, which provides with an ideal environment to compare the relative relevance of karstic and detrital groundwater discharges as a source of different elements to the nearshore ecosystem. In this study we estimate the terrestrial flux of nutrients and trace metals into the coastal waters of Majorca Island and evaluate the relative contribution of the different discharge types to the coastal dissolved inorganic nutrient and trace metal pools. Elucidating these contributions is relevant for the understanding of the temporal variations in the geochemistry of coastal waters and the consequent bottom-up controls of plankton dynamics.

Materials and Methods

Majorca Island. The Island of Majorca, located in the Western Mediterranean Sea, is the largest island of the Balearic archipelago (3.620 km^2). The industrial activity in the island is scarce, and tourism at the coastline and agriculture inland are the principal controls on the landscape. Aquifers are generally unconfined, although changes in facies and geological structures may locally impose confined and semi-confined conditions[9]. Three major types of hydrogeological formations can be distinguished in the Island; the karstic aquifers of the Serras composed by limestones from Mesozoic era; the Marinas constituted by Miocene limestones and calcarenites; and the central detrital basins filled with Cenozoic sediments (frequently Miocene limestones and calcarenites as in the Marinas) overlapped by marine and continental deposits from a period of Plio-Quaternary (Figure 1).

With the aim of comparing SGD fluxes from different settings, we divided the Majorca coastline in (1) the limestone and calcarenite aquifer discharging diffusively through sedimentary areas in small coves along the coast (Coves), (2) the limestone and calcarenite aquifer discharging preferentially through natural conduits originated from rock fissuration or karstification (Karst) and, (3) the larger detrital aquifers discharging in the large Bays (i.e. Palma, Pollença and Alcudia Bays, Figure 1C) located in the NE and SW coast of the Island (Bays). Besides of the different structural and lithological characteristics of the aquifers, these areas support different human activities. Thus, detrital basins behold intensive agriculture and large urban nuclei and tourism resorts, whereas sparse populations based on traditional dryland agriculture and smaller tourism assets settle around the coves and karst areas.

SGD flux estimation at selected sites. Comprehensive beach surveys were carried out at three coves located in the eastern coast of Majorca in November 2010 (see Figure 1). Santanyí and Romàntica are small coves where groundwater discharges to the sea are dominated by diffusive discharge through their sedimentary beaches, whereas Sa Nau is a very narrow cove in which brackish groundwater emanates through a submerged conduit located at some 30 meters from the shoreline. At each site, an onshore-offshore transect consisting in 8 to 11 points was sampled from a rubber boat to characterize the biogeochemical signal of the groundwater discharge. Surface samples were collected for the analysis of Ra, nutrients, trace metals and chlorophyll concentrations (Chl-a). Profiles of temperature and salinities down to the bottom were obtained with a CTD logger (RBR). Interstitial waters in the shore sediments were collected at different depths using

147 piezometers placed along the shoreline. For nutrients and metals analysis PVC-made
148 multi-pore piezometers[22] with acid-washed Teflon tubing were used, while we used a
149 stainless steel Retract-a-Tip (AMS) drive-point piezometer for Ra samples.

150

151 **General survey.** Surface coastal waters around Majorca Island were sampled at 41
152 coastal stations located in the near-shore at water column depths of 2-3 m, between 26
153 and 30 April 2010 (Figure 1A). The survey also included 5 open water stations located at
154 a depth of 50m along the shelf. Precipitation was almost negligible during the weeks
155 previous to the survey, except for 22 April 2010 when 26 $L \cdot m^{-2}$ were accumulated. Fresh
156 water discharges from torrents were only observed at the proximity of Na Borges torrent
157 (station 25) but fluxes from fractures and karstic conduits discharging above the sea level
158 were visible along the northern coast of the island. At each station, surface water samples
159 were obtained to determine the concentrations of nutrients, trace metals, Ra isotopes and
160 Chl-a. Surface temperature and salinity were measured at each station using a handheld
161 YSI 556 multiparameter probe. Additionally, 500 mL surface samples were obtained for
162 accurate salinity measurements. These samples were kept in cold and dark conditions
163 until measured in the laboratory with a RBR MS-315 micro-salinometer using IAPSO
164 seawater standards.

165

166 **Nutrients, trace metal and chlorophyll analysis.** Concentrations of dissolved NO_2^-,
167 NO_3^-, NH_4^+, PO_4^{3-} and SiO_2 were determined with an autoanalyzer (Alliance Futura)
168 using colorimetric techniques[23]. The accuracy of the analysis was established using

169 Coastal Seawater Reference Material for Nutrients (MOOS-1, NRC-CNRC), resulting in
170 107 ± 11 %, 107 ± 6 %, 100 ± 6 %, and 96 ± 3 % for PO_4^{3-}, NO_3^-, NO_2^- and SiO_2,
171 respectively. Limit of detection (LOD), calculated as three-times the standard deviations
172 of subsequent blank measurements, was PO_4^{3-}: 0.05 μM, NO_3^-: 0.001 μM, NO_2^-: 0.001
173 μM, and SiO_2: 0.02 μM.. Trace-metal samples were acidified to pH<2 with ultrapure
174 grade HCl (Merck) in a class-100 HEPA laminar flow hood and stored for at least 1
175 month before extraction. Dissolved (<0.22 μm) metals (Cd, Co, Cu, Fe, Mo, Ni, Pb, V
176 and Zn) were pre-concentrated by the APDC/DDDC organic extraction method[24,25] and
177 analyzed by ICP-MS (PerkinElmer ELAN DRC-e). The accuracy of the analysis was
178 established using Coastal Seawater Reference Material for trace metals (NASS-5, NRC-
179 CNRC) (obtained recoveries of 105%, 103%, 106%, 96%, 95%, 98%, 106%, 103% and
180 97% for Cd, Co, Cu, Fe, Mo, Ni, Pb, V and Zn, respectively). LOD, calculated as three-
181 times the standard deviations of subsequent blank measurements, was 6, 2, 83, 67, 275,
182 12, 8, 271 and 287 pM for Cd, Co, Cu, Fe, Mo, Ni, Pb, V and Zn, respectively. The
183 concentration of Chl-a in water samples was determined through fluorometric analysis[26].
184 The filters were extracted in 90% acetone overnight and fluorescence was measured on a
185 Turner Designs fluorometer calibrated with pure Chl-a (Sigma Co.).
186
187 **Short-lived Ra isotopes and SGD flux calculations.** Radium isotopes were measured
188 by filtering large volume seawater samples (10 L for piezometers and 60 L for coastal
189 seawater samples) through MnO_2-impregnated acrylic fiber (hereafter, Mn-fiber) at a
190 flow rate <1 L min^{-1} to quantitatively extract Ra isotopes[27]. Once in the laboratory, the
191 Mn-fibers were rinsed with Ra-free deionized water, partially dried[28] and placed in a

Radium Delayed Coincidence Counter (RaDeCC) to quantify the short-lived Ra isotopes (^{223}Ra and ^{224}Ra)[29]. Uncertainties in activities of ^{223}Ra and ^{224}Ra were estimated following Garcia-Solsona et al. (2008)[30].

In the case of the three selected beaches, the brackish SGD flux (m^3 d^{-1}) into each coastal site was calculated as:

$$SGD = f_{SGD} V / T_r$$

where f_{SGD} is the groundwater fraction in coastal waters, V is the volume affected by SGD (m^3) that, in our case, is calculated from the salinity anomaly, and T_r (days) is the residence time of coastal water (Table 2). The decay of short-lived Ra isotopes can be used to estimate the residence time of coastal waters (T_r). However, since the residence time of the studied sites is expected to some few days, the decay of the short-lived Ra isotopes is likely masked by statistical uncertainties. In these situations, a maximum water residence time can be calculated from the relative errors associated with ^{223}Ra and ^{224}Ra ($d^{223}Ra$ and $d^{224}Ra$) and the decay constants of the two Ra isotopes (λ_{223} and λ_{224}) as follows [31]:

$$T_r = \frac{\ln\left(1 - \sqrt{(d^{223}Ra)^2 + (d^{224}Ra)^2}\right)}{\lambda_{223} - \lambda_{224}}$$

The groundwater fraction (f_{SGD}) in coastal waters can be determined by using the 2-end member mixing model detailed in the following equations[32,33]:

$$f_{sea} + f_{SGD} = 1$$

$$f_{sea}\,{}^{224}Ra_{sea} + f_{SGD}\,{}^{224}Ra_{SGD} = {}^{224}Ra_{cw} e^{-\lambda_{224} T_r}$$

where f represents the relative fractions of the seawater (sea) and SGD end-members, $^{224}R_{sea}$ and $^{224}Ra_{SGD}$ are the ^{224}Ra activities in the sea and groundwater end-members,

respectively, $^{224}Ra_{cw}$ is the average activity in cove waters, λ_{224} is the decay constant of ^{224}Ra and T_r (days) is the residence time of coastal water. Here we focus on ^{224}Ra, because ^{223}Ra would provide with equivalent information to that obtained from ^{224}Ra but has larger counting errors. The concentration of $^{224}Ra_{SGD}$ was determined by extrapolating the ^{224}Ra activity vs salinity trend. Values where then normalized to a salinity of 25, which allows for comparisons among the different coves. Nutrient and trace metal fluxes at the selected coves were determined by multiplying the Ra-derived SGD flow by the respective SGD concentrations at each site obtained also by extrapolating the nutrient/metal concentrations vs salinity trend to a salinity of 25. Notice that the selection of a different salinity to characterize SGD (fresh and brackish groundwater) would considerably change the water flow but would have no effect on the next flux of chemicals derived from fresh-SGD.

We assumed that groundwater exchange only occurred through the intertidial zone of each cove, to minimize the effect of an intricate coastal geomorphology. Shoreline-normalized nutrient and trace metal fluxes ($mol \cdot d^{-1} \cdot m^{-1}$) obtained from the selected sites were used to characterize SGD-derived chemical fluxes from detrital bays (Palma Bay; from Rodellas et al., 2014[10]), coves with sedimentary discharge (Santanyí and Romàntica) and coves with karstic discharge (Sa Nau). These fluxes were multiplied by the respective coast length of Bays (35000 m), Coves (26000 m) and Karst (8000 m) in Majorca to yield the total chemical flux derived from SGD around the island.

Results and discussion

Cove surveys

As shown in Figure 2, all three surveyed coves presented lowered nearshore salinities and enhanced ^{224}Ra activities, indicative of SGD. Indeed, both variables presented very good correlations at Sa Nau and Romántica (r^2=0.91 and 0.98, respectively) and somewhat lower at Santanyí (r^2=0.61). The discharge signal was generally restricted to the waters confined within the cove and rapidly vanished to undetectable salinity anomalies and ^{224}Ra values less than 5 dpm·100L^{-1} in the shelf waters stations. These activities, although low, are higher than those recorded in previous studies[9] and in shelf water stations (^{224}Ra <3 dpm·100L^{-1}; Table 1). Most intense salinity variation occurred at Sa Nau were salinity decreased more than 1.2 units.

Salinity measurements of interstitial water at the beachface were indicative of brackish water circulation through the sediment, ranging between 10.9 and 33.7 at Santanyí and 17.8 and 32.4 at Romàntica (Table S1). ^{224}Ra measured in porewater at Santanyí and Romàntica coves (33.8 – 251.0 and 104.6-150 dpm·100L^{-1}, respectively) were considerably enriched with respect to the activities measured in the seawater at each location (Mean ± SDV; 7.2 ± 1.6 and 7.8 ± 3.2 dpm·100L^{-1}at Santanyi and Romántica, respectively). Sa Nau presented a different pattern, with interstitial ^{224}Ra activities (23.1 dpm·100L^{-1}) comparable to the range measured in cove seawater (Mean ± SDV; 29.0 ± 18.4 dpm·100L^{-1}). This lower activity in porewater cannot explain the Ra in the cove suggesting that diffusive SGD inputs through the beachface were not the dominant Ra source at this site. A visible karstic conduit discharging waters with lower salinity (i.e. 35.9) and ^{224}Ra activities exceeding 58 dpm·100L^{-1} was most likely the main groundwater pathway to the cove seawater.

256 Concentrations of inorganic nutrients (DIN, PO_4^{3-}, and SiO_2) and metals (except
257 Mo) in the interstitial waters of the three coves were larger than those in seawater (Table
258 S1). As a result of SGD, nearshore DIN and SiO_2 concentrations reached maximum
259 values of 13.5 μM (Mean ± SDV; 6.6 ± 5.5 μM) and 22.3 μM (Mean ± SDV; 8.2 ± 8.6
260 μM) at Sa Nau cove, respectively. Conversely, interstitial waters concentrations of PO_4^{3-}
261 and other metals such as Cd, Co, Cu, Ni and Pb were comparable to those in the outer
262 stations at all the studied coves, even for the Sa Nau karstic site, revealing that either
263 SGD is not a major source of these compounds or, particularly in the case of PO_4^{3-}, that
264 released concentrations are low and most probably rapidly consumed by the microbial
265 and macroalgal communities in the cove. The lack of enrichment of these compounds in
266 nearshore waters prevents estimating the SGD-derived inputs of these constituents using
267 the approach developed here. On the other hand Fe and Zn were enhanced in nearshore
268 waters allowing the calculation of their SGD-driven fluxes from the trend described by
269 their concentrations in cove waters plotted against salinity (see methods).

270 Comparison of the SGD-driven fluxes in the three systems studied and Palma
271 Beach[10] are presented in Table 2. SGD discharging through karstic conduits (Sa Nau)
272 represents a major supplier of nutrients (DIN and, particularly, SiO_2) to the coastal sea,
273 whereas diffusive SGD through large bays (Palma Beach) releases the higher fluxes of
274 dissolved Fe. This contrasting role of karstic and detrital systems is likely a consequence
275 of their differences in the degree of interaction between water and substrate in the
276 subterranean estuary. Groundwater in karstic systems is rapidly transported to the coastal
277 sea through fractures and conduits, with groundwater residence times in the aquifer being
278 generally short, limiting the interaction between groundwater and chemical compounds in

279 aquifer matrix. As a consequence, those compounds highly enriched in fresh groundwater,
280 such as DIN and SiO_2, behave conservatively along the mixing area where seawater acts
281 just as a dilution agent. Unlike karst systems, SGD through diffusive discharge allows for
282 enhanced water-solid interaction, and those constituents enriched in the fresh fraction of
283 SGD may be removed from solution[34]. However, the biogeochemical reactions occurring
284 at the subterranean estuary can also result in non-conservative additions of solutes present
285 in the aquifer solids but not particularly enriched either in groundwater or seawater[20,22].
286 These complex reactions in the subterranean estuary are likely responsible of the higher
287 trace metal inputs, particularly Fe, from the detrital bays relative to karstic systems.
288 Indeed, in Palma Bay, Fe was highly enriched (1 to 3 orders of magnitude) in the
289 subterranean estuary in relation to both fresh groundwater and seawater, what was
290 attributed to the Fe-oxide reduction due to elevated dissolved organic carbon or anoxic
291 groundwaters[10]. Aside from the differences between karstic and detritic discharge,
292 anthropogenic factors should also be taken into account in this comparison. Indeed, the
293 high SGD-derived DIN inputs from large detrital bays can be attributed to aquifer
294 contamination produced by intensive agricultural practices in those areas.

295 **Coastal water characterization**

296 The coastal stations of the survey around Majorca were classified in three clusters
297 (karst, coves and bays) according to coast geomorphology and SGD chemical properties.
298 The main challenge was separating areas of SGD through karstic conduits (karst) from
299 diffusive discharges (coves), as most karstic conduits in Majorca discharge below the sea
300 surface. Based on the results of the previous section (cove surveys), the karst stations
301 were identified from their lower salinity (<37.5) and high silicate concentration (>2 μM)

in seawater (Figure S1). As shown in Figure 1, karst stations are distributed along the coasts of the two mountain ranges bounding the NW and SE coast of the island. All the stations where groundwater fluxes from fractures and karstic conduits discharging above the sea level were visually identified are clustered as karst stations, reinforcing the appropriateness of the criterion used. Station 25, which it is not in a karstic area but was affected by surface water flow, is also clustered as karst station under this criterion.

The mean and range of all variables analyzed are presented in Table 1. Consistently with the oceanic water masses descriptions for the area[35], shelf stations presented surface salinity values within a narrow range from 38.0 to 38.1, which is indicative that shelf waters represent a sole water mass. Contrastingly, nearshore samples displayed a wide range of salinities (29.9 to 38.1). All the coastal stations presented ^{224}Ra activities above those in shelf water stations (0.7 - 2.8 dpm.100L^{-1}), with activities ranging from 3.6 to 66.8 dpm.100L^{-1} for coves with diffusive discharge, 4.1 – 35.4 dpm.100L^{-1} for karstic coves and from 2.8 to 11.1 dpm.100L^{-1} for those stations in large detrital bays (Table 1). These results are in good agreement with previously ^{224}Ra values reported along the Majorca shoreline, where SGD was identified as the main freshwater source to the coastal water[9].

Even though the seasonal thermocline was not fully developed during this season, nutrient concentrations in the shelf were characteristic of oligotrophic conditions, with low concentrations of NOx (<0.001 - 0.08 μM) and PO_4^{3-} (<0.05 – 0.07 μM) in surface waters (Table 2). As expected, mean nutrient concentrations (mainly NO_x and SiO_2) in the nearshore were higher than in shelf waters, while NH_4^+ and PO_4^{3-}, which did not display significant differences (Table 1). Nearshore enrichment was also reflected in

phytoplankton biomass measured as Chl-a, which on average doubled mean concentrations in shelf water stations (1.35 $mg.m^{-3}$ and 0.64 $mg.m^{-3}$, respectively) (Table 1).

Trace metals composition of nearshore surface waters around Majorca Island showed concentrations that are in agreement with other reported values in open waters of the Mediterranean Sea[36,37] (ranges in nM Cd: 0.34 – 0.37 ; Co: 0.14 – 0.17, Cu: 4.49 – 9.25 ; Fe: 2.38 – 3.63; Mo: 120.7 – 133.3; Ni: 3.67 – 4.19; Pb: 0.10 – 0.13; V: 12.21 – 19.04 and Zn: 2.01 – 6.56). While some metals displayed a wide range of variation, Zn and Fe (and to a lesser extent Cu), showed enhanced concentrations in several nearshore stations.

Ranges and mean concentrations of those parameters with enhanced concentrations in nearshore stations relative to outer stations (DIN, Si Fe, Zn and Chl-a) are shown in Figure 3, clustered as offshore stations, coves, karst and bays. While the range of concentrations overlap between different categories, the comparison of the clustered stations provide with some insights on the relevance of karstic and detritic systems as suppliers of different terrestrial compounds. DIN concentrations varied in a wide range, but the highest concentrations were measured in stations located in the large detrital bays. This is partially a consequence of the fertilization practices for intensive agriculture, including nutrient-rich sewage water reutilization, that have remarkably increased concentrations of NO_3^- in the aquifers of the major bays (Figure 1). Despite the high nutrient loads that these aquifers receive, depending on the groundwater transit time, a large proportion of the nitrogen discharged through the sediments can be removed from solution, either through denitrifying bacteria or matrix-derived, solid-phase electron

348 donors (like Fe^{2+} or H_2S)[38]. This may be a major difference from karstic aquifers, where
349 denitrification is minimized due to their rapid transfer times and DIN inputs from SGD
350 may be relevant even when nutrient content in the aquifer is not particularly high. On the
351 other side, Si concentrations were remarkably higher in karstic areas (Figure 3). This
352 higher concentration is likely consequence of the rapid transfer time from the aquifer to
353 the near-shore seawater and the lower geochemical reactivity in the sediments.

354 Fe was enriched at most surveyed locations, but concentrations in the large bays
355 were remarkably enhanced in relation to coves and karstic stations (Figure 3). As
356 indicated before, biogeochemical reactions in the subterranean estuary may considerably
357 reduce Fe-oxides enhancing its concentrations in SGD[10]. Zinc presented lower differences
358 among clusters, with the higher concentrations often associated to karstic and bays
359 stations, most likely related to the land-use and human activities in the different areas.

360

361 **Estimation of bulk SGD flux in Majorca and its contribution to the chemical**
362 **composition of coastal waters.**

363 The pattern observed in the selected coves (e.g. higher inputs of nutrients,
364 particularly Si, from karstic discharges and higher supply of Fe from detrital bays) seems
365 to be reproduced in the general survey around the Majorca Island. Using the flux of
366 nutrients and trace metals calculated here for the coves (both karstic and detritic) and for
367 detrital bays (Table 2), we calculated the nutrient and trace metal contribution of SGD in
368 different settings around Majorca Island. The annual loads of those elements that are
369 enhanced in nearshore waters (DIN, SiO_2, Fe and Zn) from karstic, detrital coves and

370 detrital bays, as well as the overall fluxes, are provided in Table 3. The estimated total
371 annual inputs of these chemicals to the coastal waters are: DIN: 610 10^3 kg yr^{-1}, SiO_2:
372 1400 10^3 kg yr^{-1}, Fe: 3.2 10^3 kg yr^{-1} and Zn: 2.0 10^3 kg yr^{-1}. The fluxes through the
373 detrital aquifers located in the large bays of the island represent significant fractions of
374 the total discharges of DIN (56%) and, particularly, dissolved Fe (90%). Although coves
375 with karstic discharges represent only ~10 % of the Majorca coast length, they are a
376 major source of nutrients to the coastal waters of Majorca Island, supplying 44 % and
377 74% of the total inputs of DIN and Si, respectively, derived from SGD. Our estimates
378 reveal that the nitrogen flux from karstic discharges and diffusive discharge through large
379 bays are therefore comparable, as a consequence of an interplay between the highest NOx
380 concentrations in the aquifers of large bays and the lower removal rates expected in
381 karstic-dominated discharges.

382 The large input of N and Fe in the detrital bays enhances the productivity of nearshore
383 waters, that displays higher Chl-a concentrations in the surface waters of the detrital bays
384 (Figure 1 and Table 1). Along with N and P, Fe is a key element limiting phytoplankton
385 growth in some marine environments. Even though the coastal waters of Majorca are
386 often P-limited, we suggest that the large inputs of N and Fe in the detrital bays can
387 increase phytoplankton growth because even low PO_4^{3-} levels can support primary
388 production through rapid turnover rates. Indeed, enhancement of nearshore NO_3^- and lack
389 of PO_4^{3-} can drive N-limited coastal primary production to P-limitation[4]. These conditions
390 can affect the phytoplankton community structure by favoring the proliferation of
391 organisms capable of assimilating organic phosphorous forms.

392 We are aware that many processes that occur in the subterranean estuary (e.g. physic-
393 chemical transformation, benthic respiration, redox reactions, travel/flushing times, etc.)
394 are not evaluated in this work and may influence the composition and concentrations of
395 nutrients and metal loads. Nevertheless, overall results presented here indicate that the
396 dissolved pool of nutrients (i.e. N and Si) and biogenic metals (i.e. Fe) in the coastal area
397 of Majorca Island are significantly influenced by the SGD. The large input of N and Fe
398 from the detrital aquifers enhances the productivity of nearshore waters that displays
399 enhanced Chl-a concentrations in the coastal area. Thus, the role of this significant source
400 in the cycling of chemical constituents and its effects on biogeochemical cycles of the
401 oligotrophic marine environment of Majorca Island merits further investigation.

402

403 **Acknowledgments**

404 This research has been funded by the Spanish Government projects EDASE (ref.
405 CGL2008-00047/BTE) and GRADIENTS (CTM2012-39476-C02-01). D.S.-Q. was
406 supported by the JAE-predoc program of the Spanish National Research Council (CSIC).
407 V.R. was supported through a PhD fellowship (AP2008-03044) from MICINN (Spain).
408 We thank Ana Massanet and Itziar Álvarez for assistance in field work, Gabriel Navarro
409 for the MODIS ocean color images and J. F. González (Serveis Cientificotècnics, UIB)
410 for technical support with the ICP-MS.

411 **Supporting Information Available**. Information includes values of salinity versus SiO_4
412 measured in all samples collected around Mallorca Island (Figure S1) and values of
413 salinity, Chl-a concentration, short-lived Ra activities, dissolved trace metals and

nutrients concentration, in surface waters and porewaters of three different coves of Majorca Island (Table S1). This information is available free of charge via the Internet at http://pubs.acs.org

AUTHOR INFORMATION

Corresponding Author

*Antonio Tovar-Sánchez. Department of Ecotoxicology, Ecophysiology and Biodiversity of Aquatic Systems, ICMAN (CSIC). Campus Universitario Río San Pedro, 11510 Puerto Real, Cádiz. Spain. Phone: +34 956832612. E-mail: a.tovar@csic.es

Author Contributions

A.T.-S and G.B. Conceived, designed and performed the research, analyzed data and wrote the paper. V.R., D.S.-Q, J.G.-O., P.M., A.J., J.M.L., and E.G-S performed the experiments, analysed data and wrote de paper.

The authors declare no competing financial interests.

References

(1) Behrenfeld, M. J.; O'Malley, R. T.; Siegel, D. A.; McClain, C. R.; Sarmiento, J. L.; Feldman, G. C.; Milligan, A. J.; Falkowski, P. G.; Letelier, R. M.; Boss, E. S. Climate-driven trends in contemporary ocean productivity. *Nature* **2006**, *444*, 752–755.

(2) Estrada, M. Primary production in the northwestern Mediterranean. *Sci. Mar.* **60**, *2,* 55-64 .

(3) Paerl, H. Coastal Eutrophication and Harmful Algal Blooms: Importance of Atmospheric Deposition and Groundwater as "New" Nitrogen and Other Nutrient Sources. *Limnol. Oceanogr.* **1997**, *42*, 1154–1165.

(4) Slomp, C. P.; Van Cappellen, P. Nutrient inputs to the coastal ocean through submarine groundwater discharge: controls and potential impact. *J. Hydrol.* **2004**, *295*, 64–86.

(5) Windom, H. L.; Moore, W. S.; Niencheski, L. F. H.; Jahnke, R. A. Submarine groundwater discharge: A large, previously unrecognized source of dissolved iron to the South Atlantic Ocean. *Mar. Chem.* **2006**, *102*, 252–266.

(6) Garcia-Orellana, J.; Rodellas, V.; Casacuberta, N.; Lopez-Castillo, E.; Vilarrasa, M.; Moreno, V.; Garcia-Solsona, E.; Masqué, P. Submarine groundwater discharge: Natural radioactivity accumulation in a wetland ecosystem. *Mar. Chem.* **2013**, *156*, 61–72.

(7) Giblin, A. E.; Gaines, A. G. Nitrogen inputs to a marine embayment: the importance of groundwater. *Biogeochemistry* **1990**, *10*, 309–328.

(8) Krest, J. M.; Moore, W. S.; Gardner, L. R.; Morris, J. T. Marsh nutrient export supplied by groundwater discharge: Evidence from radium measurements. *Global Biogeochem. Cy.* **2000**, *14*, 167–176.

(9) Basterretxea, G.; Tovar-Sanchez, A.; Beck, A. J.; Masqué, P.; Bokuniewicz, H. J.; Coffey, R.; Duarte, C. M.; Garcia-Orellana, J.; Garcia-Solsona, E.; Martinez-Ribes, L.; et al. Submarine Groundwater Discharge to the Coastal Environment of a Mediterranean Island (Majorca, Spain): Ecosystem and Biogeochemical Significance. *Ecosystems* **2010**, *13*, 629–643.

(10) Rodellas, V.; Garcia-Orellana, J.; Tovar-Sánchez, A.; Basterretxea, G.; López-Garcia, J. M.; Sánchez-Quiles, D.; Garcia-Solsona, E.; Masqué, P. Submarine groundwater discharge as a source of nutrients and trace metals in a Mediterranean bay (Palma Beach, Balearic Islands). *Mar. Chem.* **2014**, *160*, 56–66.

(11) Zektser, I. S.; Everett, L. G.; Dzhamalov, R. G. Submarine groundwater. **2007**, 466 pp.

(12) Swarzenski, P. W.; Izbicki, J. A. Coastal groundwater dynamics off Santa Barbara, California: Combining geochemical tracers, electromagnetic seepmeters, and electrical resistivity. *Estuar. Coast. Shelf S.* **2009**, *83*, 77–89.

(13) Polemio, M.; Casarano, D.; Limoni, P. P. Karstic aquifer vulnerability assessment methods and results at a test site (Apulia, southern Italy). *Nat. Hazards Earth Syst. Sci.* **2009**, *9*, 1461–1470.

(14) Nanni, A. S.; Roisenberg, A.; de Hollanda, M. H. B. M.; Marimon, M. P. C.; Viero, A. P.; Scheibe, L. F. Fluoride in the Serra Geral Aquifer System: Source

Evaluation Using Stable Isotopes and Principal Component Analysis. *J. Geol. Res.* **2013**, *2013*, 1–9.
(15) Garcia-Solsona, E.; Garcia-Orellana, J.; Masqué, P.; Garcés, E.; Radakovitch, O.; Mayer, A.; Estradé, S.; Basterretxea, G. An assessment of karstic submarine groundwater and associated nutrient discharge to a Mediterranean coastal area (Balearic Islands, Spain) using radium isotopes. *Biogeochemistry* **2010**, *97*, 211–229.
(16) Mejías, M.; Ballesteros, B. J.; Antón-Pacheco, C.; Domínguez, J. A.; Garcia-Orellana, J.; Garcia-Solsona, E.; Masqué, P. Methodological study of submarine groundwater discharge from a karstic aquifer in the Western Mediterranean Sea. *J. Hydrol.* **2012**, *464–465*, 27–40.
(17) Bokuniewicz, H. J. Analytical descriptions of subaqueous groundwater seepage. *Estuaries* **1992**, *15*, 458–464.
(18) Santos, I. R.; Cook, P. L. M.; Rogers, L.; de Weys, J.; Eyre, B. D. The "salt wedge pump": Convection-driven pore-water exchange as a source of dissolved organic and inorganic carbon and nitrogen to an estuary. *Limnol. Oceanogr* **2012**, *57*, 1415–1426.
(19) Li, L.; Barry, D. A.; Stagnitti, F.; Parlange, J.-Y. Submarine groundwater discharge and associated chemical input to a coastal sea. *Water Resour. Res.* **1999**, *35*, 3253–3259.
(20) Moore, W. S. The subterranean estuary: a reaction zone of ground water and sea water. *Mar. Chem.* **1999**, *65*, 111–125.
(21) Beck, A. J.; Cochran, J. K.; Saṇudo-Wilhelmy, S. A. The distribution and speciation of dissolved trace metals in a shallow subterranean estuary. *Mar. Chem.* **2010**.
(22) Beck, A. J.; Tsukamoto, Y.; Tovar-Sanchez, A.; Huerta-Diaz, M.; Bokuniewicz, H. J.; Sañudo-Wilhelmy, S. A. Importance of geochemical transformations in determining submarine groundwater discharge-derived trace metal and nutrient fluxes. *Appl. Geochem.* **2007**, *22*, 477–490.
(23) Grasshoff, K.; Almgreen, T. *Methods of seawater analysis*; Verlag Chemie, 1976.
(24) Bruland, K. W.; Franks, R. P.; Knauer, G. A.; Martin, J. H. Sampling and analytical methods for the determination of copper, cadmium, zinc, and nickel at the nanogram per liter level in sea water. *Anal. Chim. Acta* **1979**, *105*, 233–245.
(25) Tovar-Sánchez, A. 1.17 - Sampling Approaches for Trace Element Determination in Seawater. In *Comprehensive Sampling and Sample Preparation*; Editor-in-Chief: Janusz Pawliszyn, Ed.; Academic Press: Oxford, 2012; pp. 317–334.
(26) Parsons, T. R.; Maita, Y.; Lalli, C. M. *A manual of chemical and biological methods for seawater analysis*; Pergamon Press, 1984.
(27) Moore, W. S.; Reid, D. F. Extraction of radium from natural waters using manganese-impregnated acrylic fibers. *J. Geophys. Res.* **1973**, *78*, 8880–8886.
(28) Sun, Y.; Torgersen, T. The effects of water content and Mn-fiber surface conditions on 224Ra measurement by 220Rn emanation. *Mar. Chem.* **1998**, *62*, 299–306.
(29) Moore, W. S.; Arnold, R. Measurement of 223Ra and 224Ra in coastal waters using a delayed coincidence counter. *J. Geophys. Res.* **1996**, *101*, 1321–1329.

(30) Garcia-Solsona, E.; Garcia-Orellana, J.; Masqué, P.; Dulaiova, H. Uncertainties associated with 223Ra and 224Ra measurements in water via a Delayed Coincidence Counter (RaDeCC). *Mar. Chem.* **2008**, *109*, 198–219.
(31) Knee, K. L.; Street, J. H.; Grossman, E. E.; Boehm, A. B.; Paytanb, A. Nutrient inputs to the coastal ocean from submarine groundwater discharge in a groundwater-dominated system: Relation to land use (Kona coast, Hawaii, USA). *Limnol. Oceanogr.* **2010**, *55*, 1105–1122.
(32) Moore, W. S. Radium isotopes as tracers of submarine groundwater discharge in Sicily. *Cont. Shelf Res.* **2006**, *26*, 852–861.
(33) Garcia-Solsona, E.; Garcia-Orellana, J.; Masqué, P.; Rodellas, V.; Mejías, M.; Ballesteros, B.; Domínguez, J. A. Groundwater and nutrient discharge through karstic coastal springs (Castelló, Spain). *Biogeosciences* **2010**, *7*, 2625–2638.
(34) Weinstein, Y.; Yechieli, Y.; Shalem, Y.; Burnett, W. C.; Swarzenski, P. W.; Herut, B. What Is the Role of Fresh Groundwater and Recirculated Seawater in Conveying Nutrients to the Coastal Ocean? *Environ. Sci. Technol.* **2011**, *45*, 5195–5200.
(35) López-Jurado. Masas de agua alrededor de las Islas Baleares. *Bol. Inst. Esp. Oceanogra. 6*, 3–20.
(36) Yoon, Y.-Y.; Martin, J.-M.; Cotté, M. H. Dissolved trace metals in the Western Mediterranean Sea: total concentration and fraction isolated by C18 Sep-Pak technique. *Mar. Chem.* **1999**, *66*, 129–148.
(37) Agawin, N.; Tovar-Sanchez, A.; Stal, L.; Alvarez, M.; Agustí, S.; Duarte, C. Low water column nitrogen fixation in the Mediterranean Sea: basin-wide experimental evidence. *Aquat. Microb. Ecol.* **2011**, *64*, 135–147.
(38) Appelo, C. A. J.; Postma, D. *Geochemistry, Groundwater and Pollution, Second Edition*; CRC Press, 2005.

Figure Legends

Figure 1. A) MODIS ocean color image (MODerate Resolution Imaging Spectroradiometer; source NASA: http://gdata1.sci.gsfc.nasa.gov/daac-bin/G3/gui.cgi?instance_id=MODIS_DAILY_L3) for April 26, 2010 and sampling stations around Majorca Island from 26-30 April 2010 and map of sampling points at Romántica , Sa Nau and Santanyí. B) Hydrological formations of Majorca Island. C) Nitrate concentrations in wells (source IGME: http://www.igme.es/infoigme/aplicaciones/Aguas/); white dashed line delimits the main Plio-Quaternary aquifers.

Figure 2. ^{224}Ra activities and salinity anomalies in the three selected coves. Triangles indicate station position; white dotted lines represent the interface between SGD and coastal water defined by a salinity anomaly > 0.005; black dashed lines indicate the limit of the cove.

Figure 3. Box plots of DIN, Si, Fe, Zn and Chl-*a* in the different regions (Oce: Shelfwaters; Cov: Coves; Kar: Karts; Bas: Basin). Dashed line is the median concentration of each parameter in the shelf water stations. The line within the box is the median, and the boundary of the boxes indicates the 25^{th} and 75^{th} percentiles. Error bars indicate the 10th and 90th percentiles. Filled circles show outlying points.

568

569

570 **Table 1**. Mean, minimum and maximum values of salinity, short-lived Ra isotopes
571 activities, nutrients, trace metals and Chl-a concentrations observed in the coastal waters
572 of Majorca Island. According to the different structural and lithological characteristics the
573 coastline is divided in coves, karst and bays (see Material and Methods section)..

574

	Shelf waters			Coves			Karst			Bays		
	Mean	min	max	Mean	min	max	Mean	min	max	Mean	min	max
Salinity	38.05	37.99	38.10	37.86	36.75	38.10	34.19	29.92	36.83	37.76	37.17	38.10
Chl-a ($mg.m^{-3}$)	0.64	0.29	1.08	0.96	0.22	1.86	0.89	0.54	1.56	2.20	1.11	5.09
^{223}Ra ($dpm.100L^{-1}$)	0.16	0.06	0.30	0.70	0.13	5.54	1.32	0.11	3.42	0.83	0.35	1.29
^{224}Ra ($dpm.100L^{-1}$)	1.73	0.92	2.77	8.13	3.56	66.77	14.13	4.09	35.37	6.12	2.76	11.11
NO_2^-, µM	0.02	0.02	0.02	0.02	0.002	0.08	0.06	0.02	0.11	0.24	0.04	0.58
NO_3^-, µM	0.03	<0.001	0.08	2.66	0.05	20.54	5.60	0.08	28.21	3.80	<0.001	9.54
NH_4^+, µM	0.13	<0.07	0.17	0.17	<0.07	0.30	0.13	<0.07	0.20	0.17	<0.07	0.28
DIN, µM	0.17	0.09	0.23	2.84	0.12	20.69	5.77	0.22	28.30	4.08	0.08	9.89
PO_4^{3-}, µM	0.05	<0.05	0.07	0.06	<0.05	0.22	0.06	<0.05	0.14	0.04	<0.05	0.08
SiO_2, µM	0.65	0.47	0.82	1.11	0.17	2.63	6.48	2.03	16.00	0.92	0.34	1.43
Cd, nM	0.35	0.34	0.37	0.33	0.30	0.35	0.31	0.20	0.35	0.34	0.30	0.37
Co, nM	0.15	0.14	0.17	0.16	0.12	0.24	0.18	0.14	0.27	0.23	0.16	0.29
Cu, nM	7.13	4.49	9.25	7.88	3.79	15.50	9.77	3.95	20.92	7.93	3.98	10.76
Fe, nM	3.27	2.38	3.63	4.99	1.58	14.91	4.78	2.62	6.68	7.72	5.52	12.24
Mo, nM	127.63	120.75	133.25	123.51	111.86	131.24	115.43	77.17	125.69	125.64	117.33	129.90
Ni, nM	3.95	3.67	4.19	3.96	3.55	5.92	3.96	3.11	4.33	4.11	3.64	4.55
Pb, nM	0.11	0.10	0.13	0.12	0.09	0.24	0.12	0.10	0.14	0.13	0.07	0.19
V, nM	15.87	12.21	19.04	15.18	9.61	22.05	12.84	7.67	15.43	15.62	11.80	23.48
Zn, nM	3.45	2.01	6.56	4.15	1.77	9.20	6.69	2.82	11.70	5.38	3.07	8.03

575

576
577 **Table 2.** SGD-derived fluxes of nutrients and metals normalized by shore lengths in the
578 three coves and in Palma Beach.
579

580

	Santanyí		Romàntica		Sa Nau		Palma*
Type	Detrital cove		Detrital cove		Karstic cove		Detrital bay
Volume ($\cdot 10^3$ m^3)	64		84		130		31000
Maximum Residence time (d)	1.7		1.5		1.2		8.4
SGD ($m^3 \cdot d^{-1}$)	260	(40 %)	180	(40 %)	4500	(20 %)	56000
SGD/coastline ($m^3 \cdot d^{-1} \cdot m^{-1}$)	3.7	(40 %)	1.2	(40 %)	57	(20 %)	13
DIN ($mmol \cdot d^{-1} \cdot m^{-1}$)	28	(500 %)	21	(150 %)	6500	(80 %)	1900
SiO_2 ($mmol \cdot d^{-1} \cdot m^{-1}$)	29	(50 %)	22	(130 %)	13000	(40 %)	980
Fe ($\mu mol \cdot d^{-1} \cdot m^{-1}$)	250	(500 %)	610	(200 %)	500	(200 %)	4100
Zn ($\mu mol \cdot d^{-1} \cdot m^{-1}$)	2900	(40 %)	240	(500 %)	1600	(80 %)	890

581 * Rodellas et al. (2014). Uncertainties associated to SGD are ~20%

582

583

584

585

586

587 **Table 3.** Island scale estimation of nutrient and metal fluxes and proportion supplied by
588 each aquifer type. Only elements with significant enhancement are displayed.

589

590

	N	Si	Fe	Zn
Coves (mol·yr^{-1})	2.3 10^5	2.4 10^5	4.1 10^3	1.5 10^4
Karst (mol·yr^{-1})	1.9 10^7	3.7 10^7	1.5 10^3	4.7 10^3
Bays (mol·yr^{-1})	2.4 10^7	1.2 10^7	5.2 10^4	1.1 10^4
Coves (kg·yr^{-1})	3.3 10^3	6.8 10^3	2.3 10^2	9.8 10^2
Karst (kg·yr^{-1})	2.7 10^5	1.0 10^6	8.2 10^1	3.1 10^2
Bays(kg·yr^{-1})	3.4 10^5	3.5 10^5	2.9 10^3	7.4 10^2
TOTAL (kg·yr^{-1})	6.1 10^5	1.4 10^6	3.2 10^3	2.0 10^3
Coves (%)	0.5	0.5	7.1	48.3
Karst (%)	43.8	74.4	2.5	15.1
Bays (%)	55.6	25.1	90.4	36.6

591

592 **Figure 1**

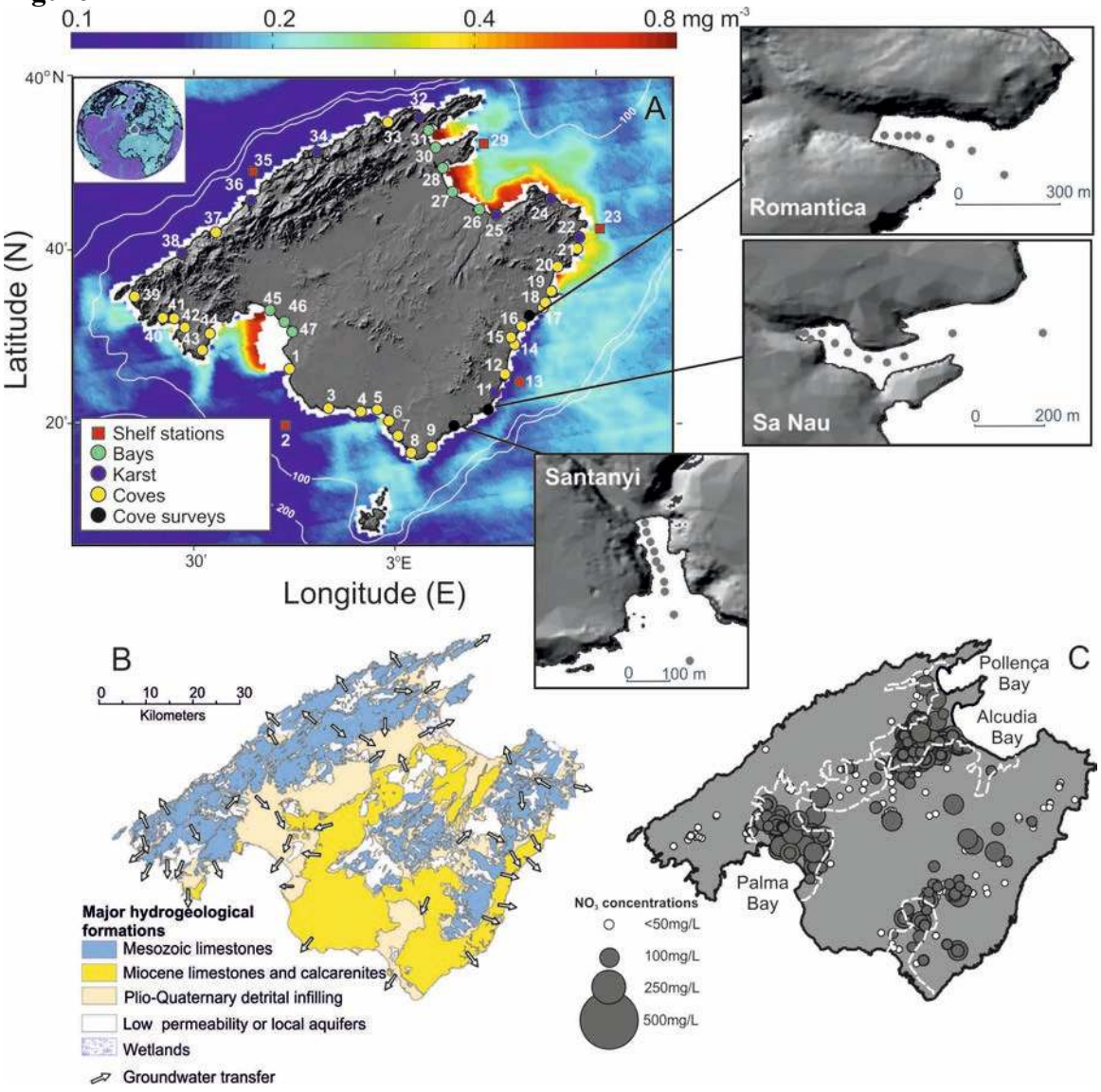

593

594 **Figure 2**

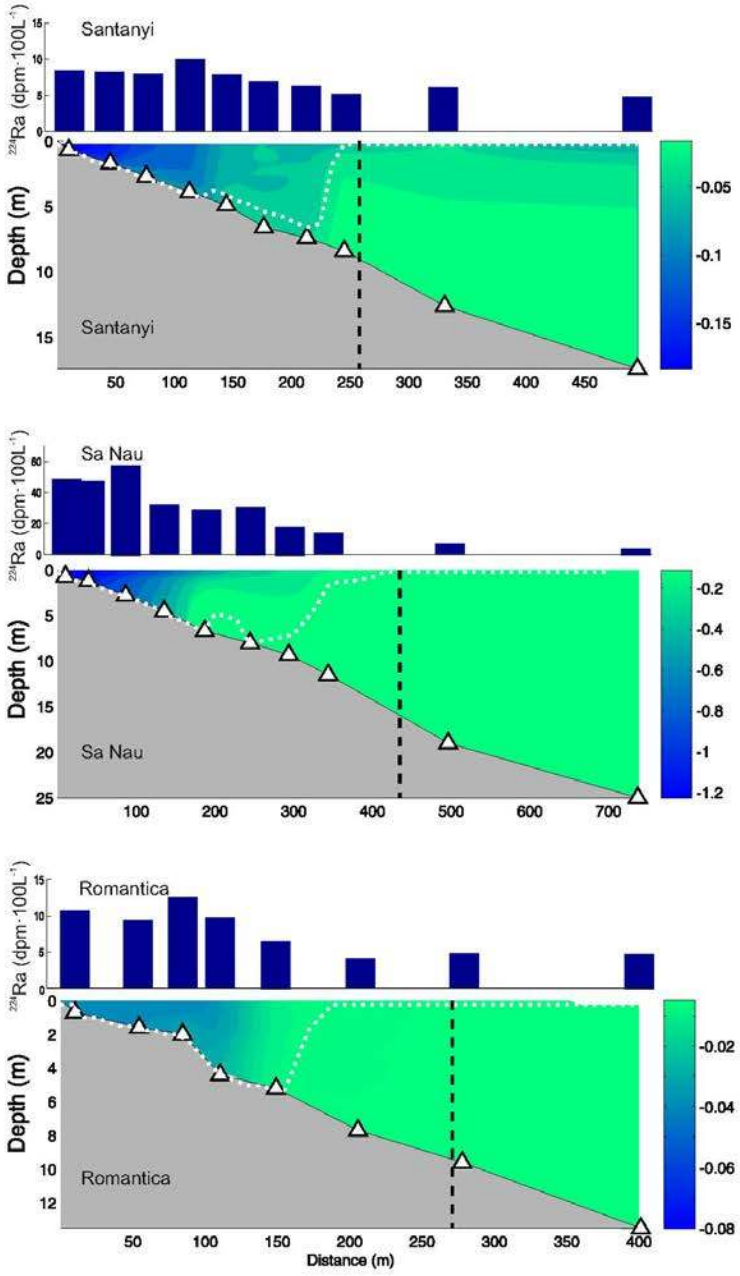

595

596 **Figure 3**

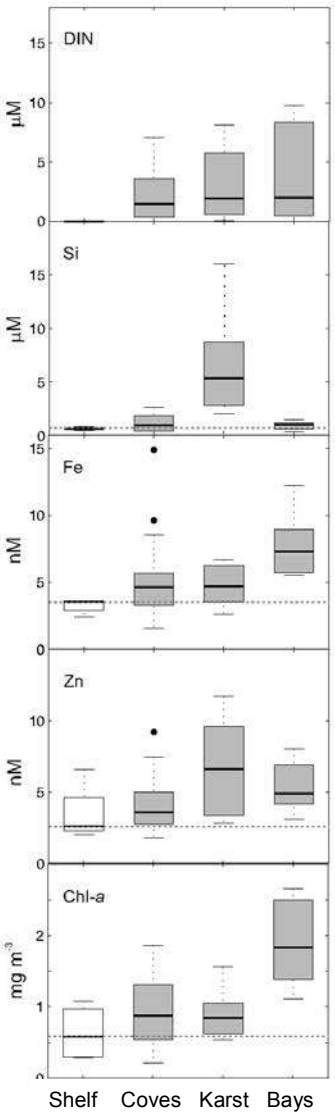

597